Processable, Electroactive, and Aqueous Compatible Poly(3,4-alkylenedioxypyrrole)s through a Functionally Tolerant Deiodination Condensation Polymerization

Ryan M. Walczak, James K. Leonard, and John R. Reynolds*

The George and Josephine Butler Polymer Research Laboratory, Center for Macromolecular Science and Engineering, Department of Chemistry, University of Florida, Gainesville, Florida 32611

Received July 17, 2007; Revised Manuscript Received November 7, 2007

ABSTRACT: We present a method for the synthesis of soluble and processable 3,4-alkylenedioxypyrrole (XDOP)-based conjugated polymers via an iododecarboxylation−deiodination polymerization methodology. Polymerization to the respected PXDOP derivatives of suitably high molecular weight (3.8−14.2 kDa vs polystyrene as measured by GPC) was achieved by either heating the neat monomers for a few hours or allowing them to remain at room temperature for several days. A family of four polymers was synthesized and characterized optically and electrochemically. Polymer solutions were transparent in the visible in their neutral states, red in their partially oxidized states, and grayish-green in their heavily oxidized states. Electrochemical measurements of cast films show that all redox processes occur at low potentials (ca. 0 V vs the Fc/Fc^+), similar to electrodeposited films. Polymers spray-cast as films onto ITO exhibited high band gaps above 3.0 eV along with stable UV and near-IR electrochromism in organic solvents with almost no change in the visible. An amphiphilic polymer functionalized with oligoethoxy substituents exhibited enhanced electrochemistry in aqueous electrolyte and high-contrast electrochromism with respect to the nonpolar functionalized polymers in the visible and near-IR.

Introduction

With increasing interest in the use of conjugated polymers in widespread applications, it has become necessary to formulate new materials that are processable, soluble, and able to be produced on a large scale.[1] While extensive literature exists on the preparation of a number of soluble and processable conjugated polymers, there is little information published on the scaled-up synthesis of soluble and processable polypyrrole or poly(3,4-alkylenedioxypyrrole) (PXDOP) derivatives.[2,3] The group of Merz demonstrated that a free-standing film of poly(3,4-dimethoxypyrrole) could be synthesized by electrolysis,[4,5] but the subsequent material was not soluble or processable. The group of Kim has successfully prepared a soluble PXDOP derivative oxidatively with $FeCl_3$, but the material was not thoroughly characterized and no information as to its electrochemistry was presented.[2]

Research presented here utilizes a new method for the chemical synthesis of soluble and processable PXDOP derivatives via a deiodination polymerization methodology. This route makes use of the iododecarboxylation methodology developed by the Merz group[6] and later explored by our group[7] in small molecule synthesis. We have now found that diiodinated XDOP derivatives undergo rapid reaction in bulk, subsequently forming high molecular weight doped conjugated polymer. This polymerization bears a resemblance to the work published by the Wudl group on the solid-state polymerization of 2,5-dibromo-3,4-ethylenedioxythiophene (dibromo-EDOT), which was found to occur due to the orientation of the halogen termini, but in the present instance the polymerization occurs from the liquid state.[8] This article demonstrates the successful polymerization of diiodinated XDOP derivatives from both liquid and solid monomers and that these soluble and processable polymers are highly electroactive and chromic materials.

* Corresponding author. E-mail: reynolds@chem.ufl.edu.

Results and Discussion

Monomer Synthesis. Scheme 1 describes the synthesis of four PXDOP derivatives. Adapted from previously reported procedures,[7,9−11] synthesis began with ethyl bromoacetate: compounds **1a** and **1b** were synthesized from their respective amines. Subsequent formation of the ester protected dihydroxypyrrole intermediates **2a** and **2b** was accomplished by condensation with diethyl oxalate in methanol or ethanol under basic conditions followed by acidic work-up. Williamson etherification with the appropriate halide or tosylate **3a**−**d** produced annulated compounds **4a**−**c** and the dialkylated derivative **4d** in moderate to good yields. It was found that these esters could be stored for prolonged periods of time (several years) without noticeable decomposition. The esters were then saponified under basic conditions to afford the diacids **5a**−**d** after acidic work-up. The iododecarboxylation of diacids **5a**−**d** was performed by dissolving them into aqueous potassium carbonate solution followed by the dropwise addition of KI_3 solution. The diiododinated monomers **6a**−**d** were isolated in high yields after work-up as solids or viscous oils. Polymerization to the respected PXDOP derivatives was achieved by either heating the diiodo derivatives at 40 °C for a few hours or by allowing them to remain at room temperature for several days. After dissolving into a THF/hydrazine mixture (the hydrazine used to dedope the polymer and quench remaining iodine) and precipitating into a nonsolvent, it was found that the polymers were of suitably high molecular weight (3.8−14.2 kDa vs polystyrene as measured by GPC) for subsequent structural, electrochemical, and optical characterization.

Pendant group substituents for polymers **7a**−**d** were chosen to demonstrate property control with the following logic: (1) Alkyl substitution onto the alkylene bridge of polymer **7c** was expected to induce high solubility in common organic solvents (conceptually, as our group has previously demonstrated for dioxythiophene derivatives[12−15]). (2) Branched alkyl substitution

10.1021/ma071589q CCC: $40.75
Published on Web 01/04/2008

Scheme 1[a]

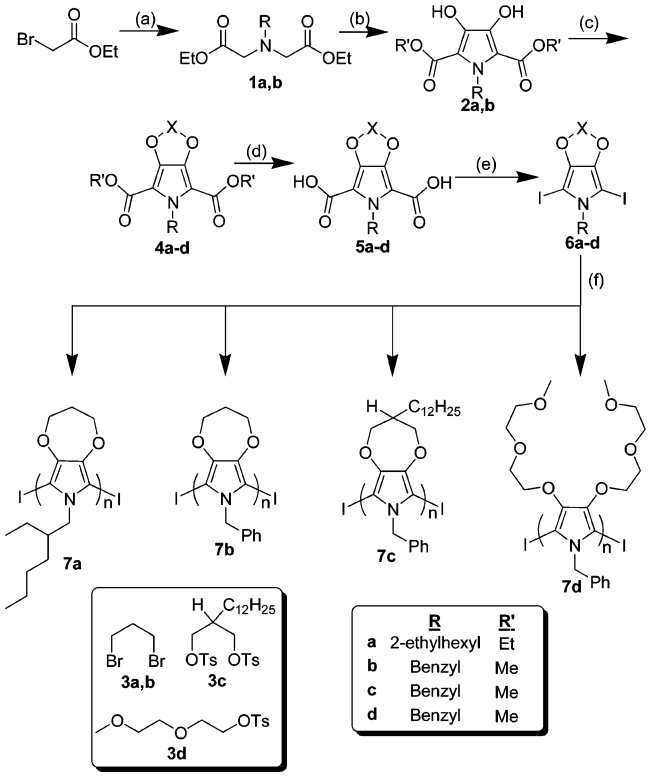

[a] (a) R-NH_2/K_2CO_3/DMF, 79−85%; (b) NaOR′/R′OH/diethyl oxalate, 48−67%; (c) **3**/K_2CO_3/DMF, 33−78%; (d) NaOH/H_2O/acetone (or EtOH)/reflux, 80−100%; (e) KI/I_2/H_2O, 63−100%; (f) bulk polymerization.

onto the *N*-position on polymer **7a** was expected to have the same effect. (3) Polymer **7b** was of interest because, unlike the other monomers **6a,c,d**, which were viscous oils, monomer **6b** was a solid at room temperature. (4) The oligoethoxy groups on polymer **7d** were chosen to enhance aqueous compatibility and ion incorporation into the polymer matrix.

Autocatalyzed Polymerization. The discovery of this polymerization reaction was serendipitous in that, during the attempted isolation of compound **6a** for prospective use in metal-mediated coupling reactions, it was observed that after a short period of time (30 min) the purified yellow oil became red and after a few hours, black. After remaining for 1 week at room temperature, it was found that the once viscous oil became a shiny black solid in the bottom of the flask. This polymerization was believed to entail the coupling of monomer accompanied by the release of elemental iodine. Because neutral PXDOP derivatives are known to possess band gaps in excess of 3.0 eV, and thus exhibit minimal absorbance in the visible region,[3,11] it was believed that the deep black color of the polymer was a result of the iodine condensate oxidatively doping the polymer, thus increasing its absorbance in the visible. After treatment with hydrazine, it was found that the material became yellow and highly soluble in THF. After precipitation into methanol and redissolving into THF, gel permeation chromatography (GPC) analysis confirmed that it was indeed a polymer (M_n = 7600 Da, PDI = 1.93), and it became evident that this method could be useful in the synthesis of soluble and processable PXDOP-based conjugated polymers. To gain insight into the optimal polymerization conditions, and perhaps to determine a qualitative polymerization reaction pathway, several polymerization experiments were performed under various conditions.

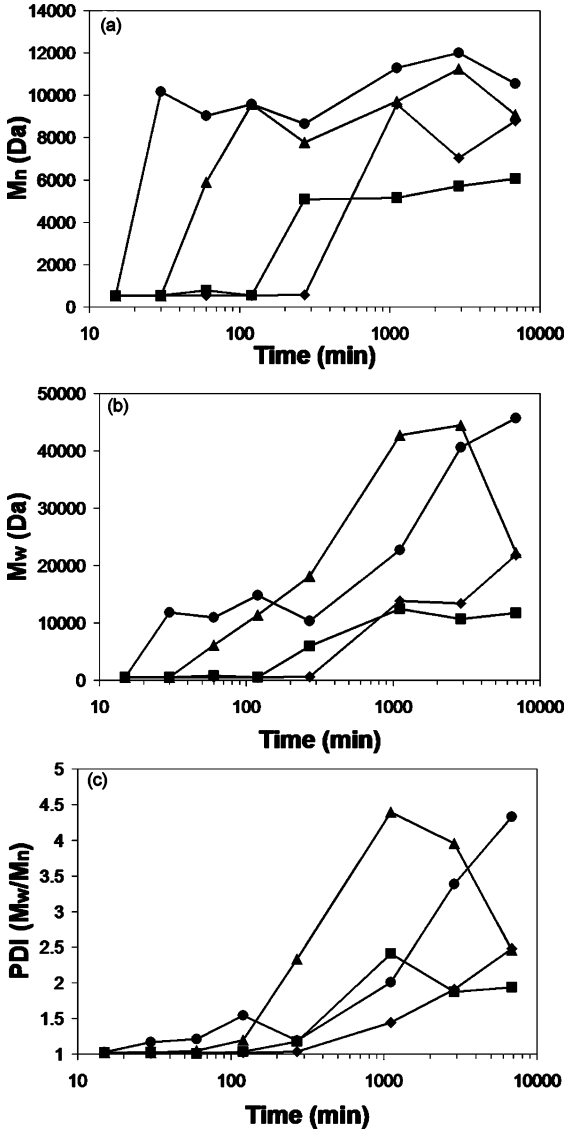

Figure 1. Polymerization of compound **6a**, in bulk, at various temperatures for 4.5 days. Aliquots were taken at various time intervals and prepared for GPC analysis by treatment with hydrazine, dissolving into THF, and filtering to remove insoluble matter. (a) Number-average molecular weight (M_n) evolution. (b) Weight-average molecular weight (M_w) evolution. (c) Polydispersity index (PDI) evolution. Key: (◆) 5, (■) 23, (▲) 40, and (●) 60 °C.

Solution vs Bulk Polymerization. To study the effect of solvent on the polymerization reaction, THF was used due to its known affinity for the previously described polymer **7a**. This experiment was performed by simultaneously placing four equal portions of **6a** under argon and subjecting them to different polymerization conditions for 1 week, as represented in Table 1. At the end of each experiment, the reactions were worked up by adding a solution of 1% hydrazine in THF, precipitation into methanol, and dissolving into THF; this was followed by GPC characterization. It can be seen that when the monomer was prepared as a 0.20 M solution in THF, polymerization did not occur, even at 60 °C for 1 week. This lack of polymerization in THF poses a great advantage because it presents a storage medium in which the monomer could be saved for a period of time without the risk of polymerization.

It was also observed that the bulk polymerization at 60 °C produced a polymer with visibly poorer quality (pale yellow vs dark brown) than that polymerized at 23 °C, and the molecular weight was lower. With these results in hand, it became evident

Table 1. THF Solution vs Bulk Polymerization of Compound 6a

temp (°C)	solvent (molarity)	M_n (Da)	M_w (Da)	PDI	polymer appearance after treatment with hydrazine
23	bulk	11400	13300	1.16	soluble, pale yellow
	THF (0.20 M)	monomer	monomer		liquid monomer
60	bulk	5900	9100	1.55	mostly insoluble, dark brown
	THF (0.20 M)	monomer	monomer		liquid monomer

Table 2. Data for the Polymerization of 6a at Various Temperatures

reaction temp (°C)	induction period (min)	work-up fraction	M_n (Da)	M_w (Da)	PDI	% yield of fraction
5	690 ± 420	precipitate	10900	24400	2.24	45
		filtrate	2700	4500	1.67	19
					total yield:	64
23	195 ± 75	precipitate	8000	13000	1.60	50
		filtrate	2000	3000	1.38	29
					total yield:	79
40	30 ± 15	precipitate	13000	30000	2.29	26
		filtrate	2300	3300	1.42	25
					total yield:	51
60	15 ± 15	precipitate	8500	16400	1.94	61
		filtrate	3300	4200	1.26	27
					total yield:	88

that a study of the temperature dependence of the polymerization of neat monomer was necessary for the understanding of the polymerization process as well as to develop an optimized synthetic procedure.

Temperature Dependence of the Polymerization Reaction. To study the temperature dependence, side-by-side bulk polymerizations were performed under otherwise identical conditions. Samples of the reactions were taken at various time intervals and, after work-up with hydrazine/THF, were characterized via GPC. Figure 1 shows the molecular weight evolution as a function of polymerization time. It is clear that the M_n reached a limiting value at short periods of time and bears resemblance to the conversion plots for the solid-state polymerization of dibromo-EDOT.[8] First, it is evident that there is an induction period for the polymerization which decreases with increasing temperature. Subsequently, the polymerization ensues and each sample attains a high molecular weight. Interestingly, the samples that were polymerized at 5 °C seem to be of higher molecular weight than those polymerized at 23 °C. The molecular weight fluctuations observed are most likely due to several factors, including small sampling aliquots and polymer solubility (the samples polymerized at higher temperatures contained ~25% insoluble material, and only the soluble fractions were measured by GPC).

Also observed was that the M_w and PDI continued to increase after the M_n leveling effect occured. This broadening, which was exacerbated with increased polymerization temperature, was likely due to either the continued polymerization via the iodine end groups or some manner of free-radical decomposition or cross-linking initiated by the homolytic bond cleavage of elemental iodine. It is not clear as to whether the polymer quality (e.g., solubility and color) degraded as a function of this broadening, but because the molecular weight leveling occurred on a small time scale compared to that of the broadening of polydispersity, shorter reaction times may produce better quality samples without sacrifice of chain length. On the other hand, this shortening of reaction time to improve sample quality may reduce the yield of soluble and processable polymer that would be recovered after work-up.

As noted, an induction period was observed that varied with temperature. The induction period values were taken as the halfway point between the times immediately before and after the observed jump in M_n. As shown in Table 2, this induction period decreased as a function of increasing temperature. It was also observed that the induction period was circumvented by the addition of a crystal of iodine to the monomer bulk to affect an immediate polymerization. The molecular weight values in Table 2 were obtained by dissolving the polymer in THF followed by precipitation into methanol (the "precipitate" in Table 2). The methanol was removed in vacuo, and the remaining solid residue (the "filtrate" in Table 2) was characterized alongside that of the precipitated fraction. Percentage yields were calculated as the moles of pyrrole rings obtained divided by the moles of pyrrole rings initially used in the reaction. The yield value (Y) is based on the number-average molecular weight and was determined by the following equation:

$$Y\,(\%) = \frac{m_p M_0 (M_n - 2M_E)}{m_0 M_n (M_0 - 2M_E)} \times 100$$

where m_p is the mass of the polymer, M_n the number-average molecular weight of the polymer, M_0 the monomer molecular weight, M_E the end-group molecular weight (in this case it is iodine, 126.9 g/mol), and m_0 the initial monomer mass. This calculation method is employed due to the relatively large mass of the iodine end groups, which were not ignored, as is typically done in yield determination. It can be seen that the precipitation procedure was an effective way to remove low molecular weight polymer from the material because, as observed in Table 2, the low molecular weight fractions were soluble in methanol, whereas the higher molecular weight fractions were not.

Time Dependence of Molecular Weight Distribution and Yields. Whereas the 23 °C polymerization exhibited an induction period on the order of 3 h and the 60 °C polymerization on the order of 15 min, the 40 °C sample induction period was at an intermediate value and thus posed the most convenient temperature at which time dependence studies could be examined. Aliquots of monomer **6a** were transferred to sealed vials and simultaneously immersed into a 40 °C bath. The vials were subsequently removed at 10 min intervals, and the reactions were quenched with THF/hydrazine and directly characterized by GPC without precipitation.

Figure 2 shows the time-dependent molecular weight distribution for the polymerization reaction as described above. It can be seen that the 30 ± 15 min induction period from the temperature dependence experiment was reproducible by the sudden emergence of a peak at ca. 10 000 Da after 40 min, with only a trace of high polymer observed at 20 and 30 min. Interestingly, a small amount of oligomer (M_n < 2000 Da) was

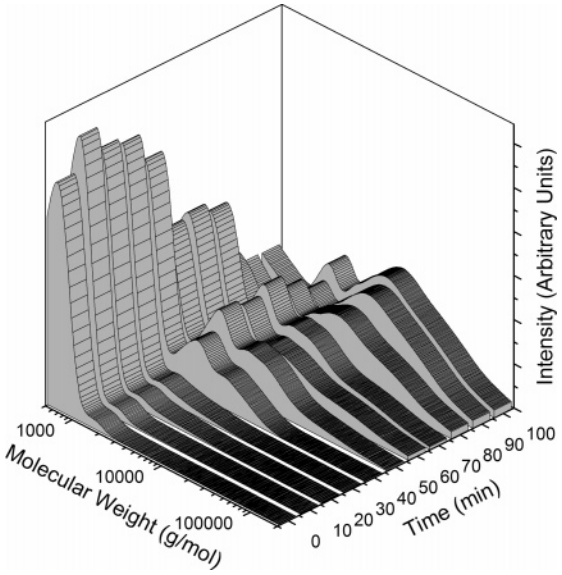

Figure 2. Molecular weight distribution as a function of time for the deiodination polymerization of compound **6a** at 40 °C.

observed for the $t = 0$ sample (immediately quenched after synthesis and work-up), indicating that a low degree of polymerization occurred during the workup step. As expected, the intensity of this peak did not change until the 40 min time interval. It is plausible that if oligomers were formed during the decarboxylation reaction, and all subsequently released elemental iodine was quenched during the work-up and purification step, this small trace of oligomer would not cause an initiation of the polymerization (the reason for this will be clarified in the next section, where a hypothetical polymerization reaction pathway is proposed).

After the induction period, it can be seen that GPC peaks corresponding to high molecular weight polymer emerged with a concurrent decrease in intensity of the lower molecular weight peaks. It is unclear as to the origin of the observed multimodal molecular weight distribution, but it may be explained through a heterogeneous polymerization pathway. If non-simultaneous initiation events occurred, and the kinetics of initiation were slow, then the observed multimodality may have been an artifact of an inhomogeneous polymerization reaction pathway. This is in contrast to a typical free-radical polymerization, where initiator is homogeneously dispersed throughout the sample. Indeed, it was observed visually during these polymerizations that small dark spots formed in the colorless bulk monomer, and polymerization would proceed out in all directions from that spot. These observations are consistent with the proposed polymerization reaction pathway that will be described later.

Practically, polymers with complex molecular weight distributions, especially those containing a large amount of low molecular weight material, are fractionated to reduce polydispersity. To characterize the effect of polymerization time on the yield, polydispersity, and molecular weight after fractionation, aliquots of **6a** were polymerized in sealed vials at 40 °C, and each vial was removed at a specific time interval, quenched by the addition of THF/hydrazine followed by precipitation into methanol. As shown in Table 3, at short polymerization times (less than 1 h) no polymer was effectively isolated via precipitation. After 1 h, polymer was isolated with inconsistent yields, but with high M_n which varied between 15 200 and 21 400 Da, with an increasing PDI as a function of time. It was also observed that the molecular weight distributions of the fractionated samples were unimodal, indicating that precipitation was an adequate method for narrowing the polydispersity.

Table 3. Molecular Weights, Distributions, and Yields after Precipitation for the Polymerization of Compound 6a at 40 °C

sampling time (min)	initial monomer mass (mg)	isolated polymer mass (mg)	M_n (Da)	M_w (Da)	PDI	% yield
27	290	0				0
43	254	0				0
64	253	100	21 400	37 500	1.75	79
83	239	32	18 900	44 000	2.34	27
106	263	128	15 200	44 700	2.94	97

Proposed Reaction Pathway for the Deiodonation Polymerization. The reaction pathway proposed by the Wudl group for the solid-state polymerization of dibromo-EDOT states that as EDOT is oxidatively polymerized by $FeCl_3$ ($E^0 = 0.77$V), then it could also be polymerized by Br_2 ($E^0 = 1.07$ V).[8] As such, the polymerization occurs by an oxidation of dibromo-EDOT to its radical cation by elemental bromine followed by radical addition to another monomer moiety, followed by the rearomatization and regeneration of the catalytic bromine; Br_3^- serves as the counterion for the resulting radical cation. Since this Br_3^-/oxidized thiophene couple is in thermodynamic equilibrium with the elemental bromine/neutral thiophene couple, it can be expected that oxidative doping by bromine would compete with condensation of free bromine inside the reaction vessel. Indeed, when a solid-state polymerization of dibromo-EDOT was performed in a closed vial, a large amount of elemental bromine was observed to form. However, they are clear to note that the polymerization reaction is favorable because the crystal structure allowed for proximal bromide end groups to initiate the reaction.

The reaction pathway for the deiodination polymerization is thought to occur via a similar route. One complexifying factor is that the PXDOP family of polymers is easily doped by elemental iodine vapor. This was evident from the fact that the resulting polymers were deep black in color, indicating the polymer derivatives were in their doped form. Similarly, the crystals of dibromo-EDOT observed by Wudl (which were observed to be deep blue in color) indicated that the PEDOT was at least partially in its undoped form. Figure 3 illustrates the proposed reaction pathway for the deiodination polymerization reaction of the XDOP derivatives in the formation of a hexamer. First, an initiation event may occur as a homocoupling of two monomers followed by the simultaneous rearomatization and release of elemental iodine into the system. Thus, the reaction is thought to be autocatalytic.

A monomer could then be oxidized to its radical cation by elemental iodine, with the concomitant release of an iodine radical (which may oxidize another monomer or couple to form diiodine), and is counterbalanced with an iodide anion. The radical cation can then couple with another monomer, forming the radical cation dimer, followed by the release of elemental iodine (this elemental iodine can then oxidize monomer). The radical cation dimer can then react with another monomer, producing the trimer radical cation, followed by the release of more elemental iodine. As shown in the resonance form for the trimer radical cation, this radical cation is not necessarily delocalized along the entire polymer chain. More chain propagation can occur, or as shown in this example, a hexamer is formed by the coupling of two radicals followed by the release of elemental iodine. As each reaction occurs, one molecule of elemental iodine is released, producing an acceleration of the autocatalytic effect. Polymeric species can be reoxidized by elemental iodine to the p-type doped state, and propagation can proceed to produce longer polymer chains by the same reaction pathway. The content of iodine in the dedoped polymer, as

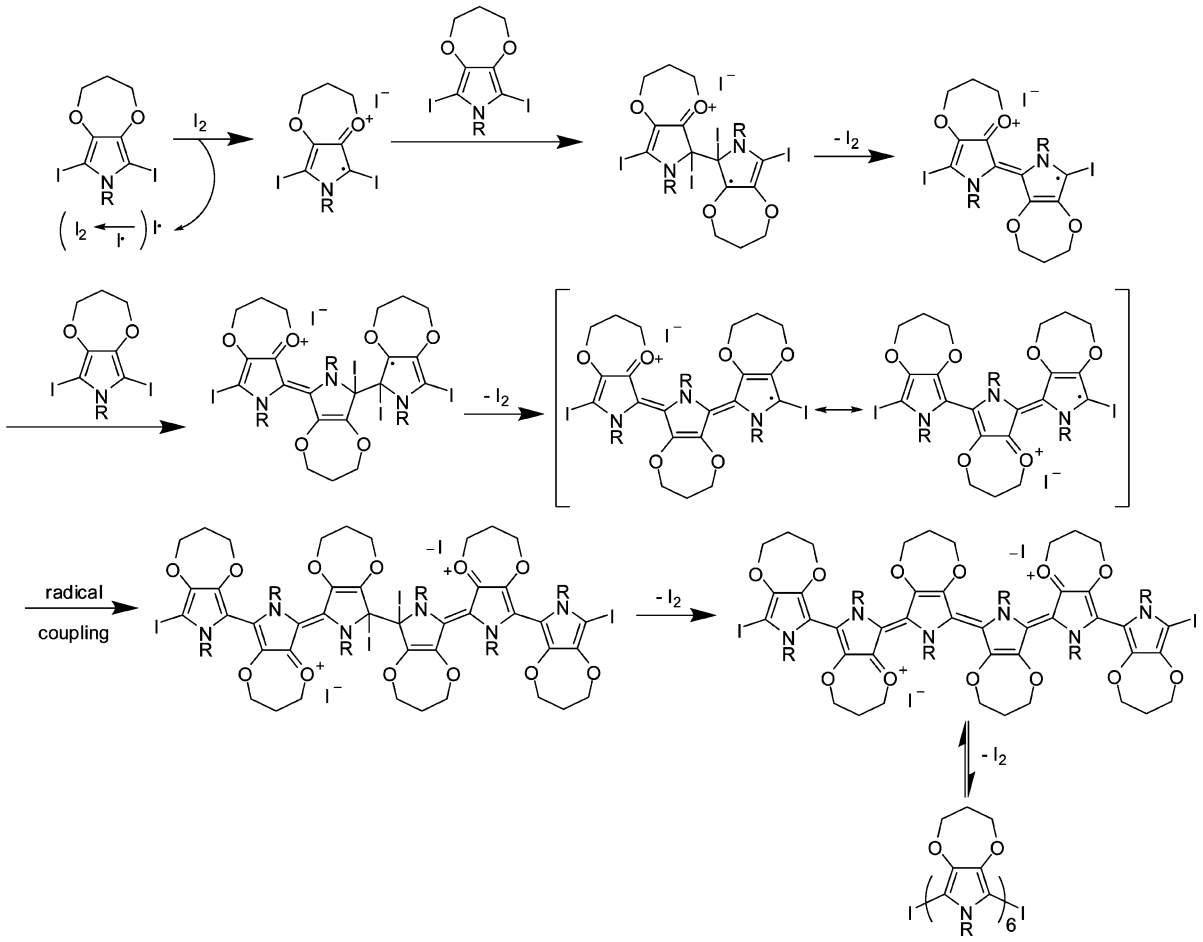

Figure 3. Proposed reaction pathway for the deiodination polymerization.

measured by combustion analysis, suggests molecular weight values that are much higher than what was measured by GPC. Therefore, we believe that the combustion analysis results are not an accurate way of determining molecular weight data. However, the low iodine content in the polymer suggests that either the iodine end groups were removed in the hydrazine quenching step or some manner of chain termination was the cause of the observed molecular weight leveling effect.

Soluble *N*-Alkylated PXDOPs via Deiodination Polymerization. It is clear that this new polymerization method can be used to synthesize a large library of PXDOP-based conjugated polymers. Furthermore, the conditions of polymerization are more tolerant of functional groups that may react under harsher conditions (such as $FeCl_3$ oxidative polymerization) or render the material difficult to purify. Additionally, as stated above, the XDOPs with esters at the 2- and 5-positions can be stored for prolonged periods of time; these esters can then be hydrolyzed and converted to the monomeric form in two simple steps. To investigate the potential utility of the deiodination polymerization toward the synthesis of a variety of PXDOP derivatives, a family of four diiodinated monomers, whose syntheses are described above in Scheme 1, were polymerized under various conditions (see Supporting Information). Table 4 summarizes the molecular weight results for polymers **7a**−**d** showing that, with the exception of **7b**, all polymers were of relatively high molecular weight, with M_n values in the range of ca. 9000−14 000 Da, which corresponds to 20−50 repeat units. Polymer **7b** was of lower molecular weight, perhaps because it was polymerized from a solid monomer, but the value of 3800 Da corresponds to a polymer structure of 16 repeat units and most likely was a material with saturated electrochemical and optical properties; therefore, it was still considered to be a sufficient material for electrochemical studies.

Table 4. Molecular Weight Results for the PXDOP-Rx Synthesized via Deiodination Polymerization

polymer	M_n (Da)	M_w/M_n	X_n
7a	14200	1.75	56
7b	3800	1.59	16
7c	8700	1.81	21
7d	10300	1.68	26

As the four polymers contained different pendant groups, they are expected to exhibit different materials properties. The racemic branched chain *N*-ethylhexyl group of polymer **7a** was expected to prevent π-stacking and enhance the polymer solubility. Indeed, it was observed that this polymer is soluble in a large variety of organic solvents but insoluble in hexane and water. As such, hexane was an excellent nonsolvent for precipitation and, as described above, effectively removed low molecular weight fractions. Monomer **6b** was a solid at room temperature, and the efficacy of polymerization was investigated. Polymer **7b** was successfully synthesized in the solid state, but the reaction time was an order of magnitude greater than that of the polymerization of the liquid compound **6a**. The *N*-benzyl group on polymer **7b** was expected to affect the polymer properties, possibly through an enhanced mode of π-stacking. Dissolution into dichloromethane (DCM) followed by precipitation of this polymer into hexane did not effectively remove low molecular weight fractions from the polymer, but subsequent precipitation into methanol was successful in narrowing polydispersity. Monomer **6c**, a liquid, and *N*-substituted with a benzyl group contained a prochiral center on the alkylene bridge via the monosubstitution of a long-chain dodecyl group. The

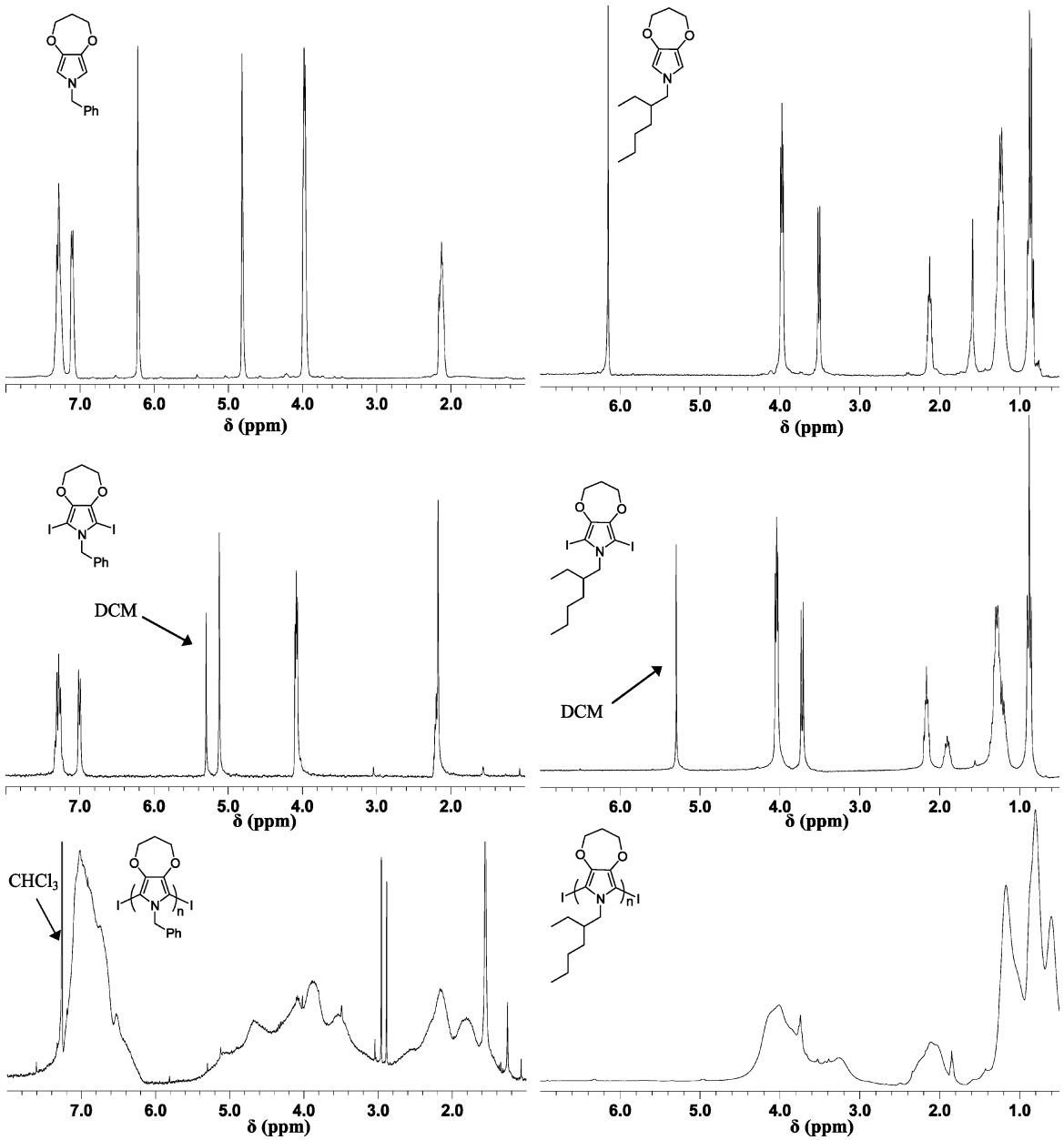

Figure 4. ^{1}H NMR (300 MHz in $CDCl_3$) spectra of monomers and polymers: (a) ProDOP-*N*-Bn, (b) **6b**, (c) **7b**, (d) ProDOP-*N*-EtHx, (e) **6a**, and (f) **7a**.

resulting polymer **7c** was thus regioasymmetric and was easily precipitated from DCM into hexane. It will be seen that this polymer, compared to **7b**, exhibited facile electrochemical switching, presumably due to enhanced polymer interaction with solvent and electrolyte. The introduction of straight-chain triethylene glycol monomethyl ether chains onto the PXDOP core (polymer **7d**) was expected to enhance aqueous switching through its hydrophilicity and affinity toward metal cations. Because of this expected affinity, it is believed that oxidative polymerization with $FeCl_3$ would produce a polymer with coordinated metal cations that would be difficult to remove in purification, making deiodination polymerization a better method for synthesizing metal-free polymer. Liquid monomer **6d** was polymerized over 4 days at room temperature to yield, after hydrazine reduction and precipitation from DCM into hexane, a tacky, dark mass which possessed a high M_n, a narrow polydispersity, and a clean ^{1}H NMR with broad peaks.

Figure 4 shows the NMR spectra of polymers **7a** and **7b** along with their diiodinated and non-iodinated monomeric analogues. It can be seen that slight shifts occur in the monomer when substituted with the iodine groups, presumably due to their electron-withdrawing character. More noticeably, polymers **7a** and **7b** exhibited broad peaks, probably due to long relaxation times, and a complex polymer solution conformational distribution. Regardless, peaks attributed to specific functional groups, such as the benzyl group at ca. 7 ppm in polymer **7b** and the ethylhexyl group at ca. 1 ppm in polymer **7a**, are consistent with the monomers.

Polymer Solution Oxidation. To study the evolution of the optical spectra and color during solution oxidation, the polymers were dissolved into DCM and treated with 2−10 μL aliquots of a solution of 1 mM nitrosonium hexafluorophosphate in DCM. For example, as shown in Figure 5, a solution of 13 μg/mL of polymer **7a** in DCM exhibited an especially strong UV absorption with a λ_{max} at 315 nm, corresponding to a molar absorptivity of $\sim 5.1 \times 10^5$ mol^{-1} cm^{-1} (per repeat unit). This polymer solution was completely transparent in the visible when in its neutral state, and even with an order of magnitude higher

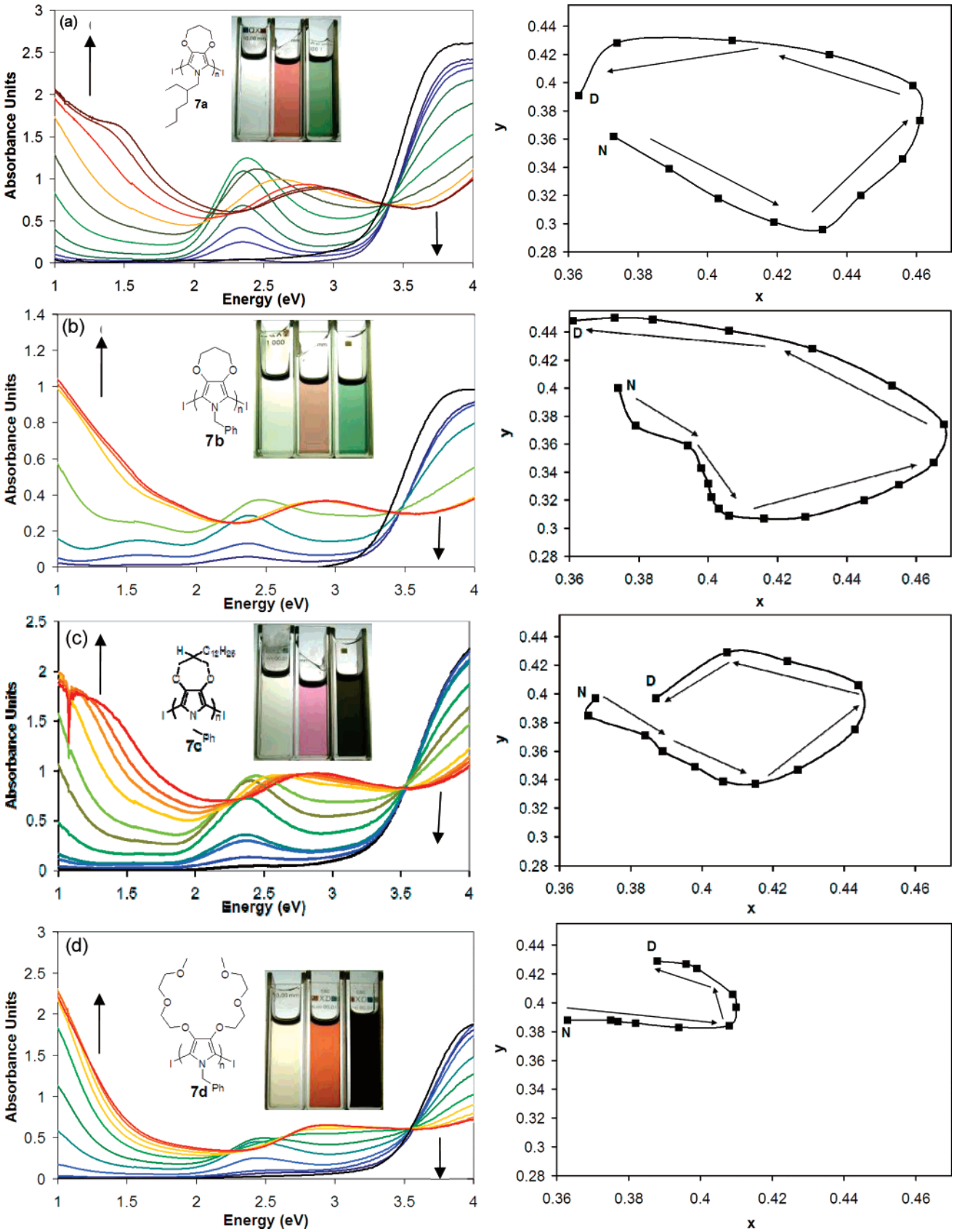

Figure 5. Solution oxidation spectra with digital photographs (left) and colorimetry (right) of polymer solutions with 2 μL aliquots of 2.5 mM $NOPF_6$ in DCM: (a) **7a**, 13 μg/mL; (b) **7b**, 19 μg/mL; (c) **7c**, 13 μg/mL; (d) **7d**, 130 μg/mL. Arrows indicate direction of the transitions from neutral polymer, N, to doped polymer, D. Solution concentrations for colorimetry and digital photos were 10 times that of the spectroscopy solutions.

concentration (0.52 mM in repeat units), the polymer solution exhibited only a very slight yellow color.

As evidenced by the photographs in Figure 5, upon oxidation with $NOPF_6$, a color change of each solution from transmissive to red was observed with the concomitant emergence of a peak at ca. 550 nm, which can be attributed to the formation of delocalized cation radicals (polarons) along the π-conjugated backbone. Note the arrows on the spectra in Figure 5 show the

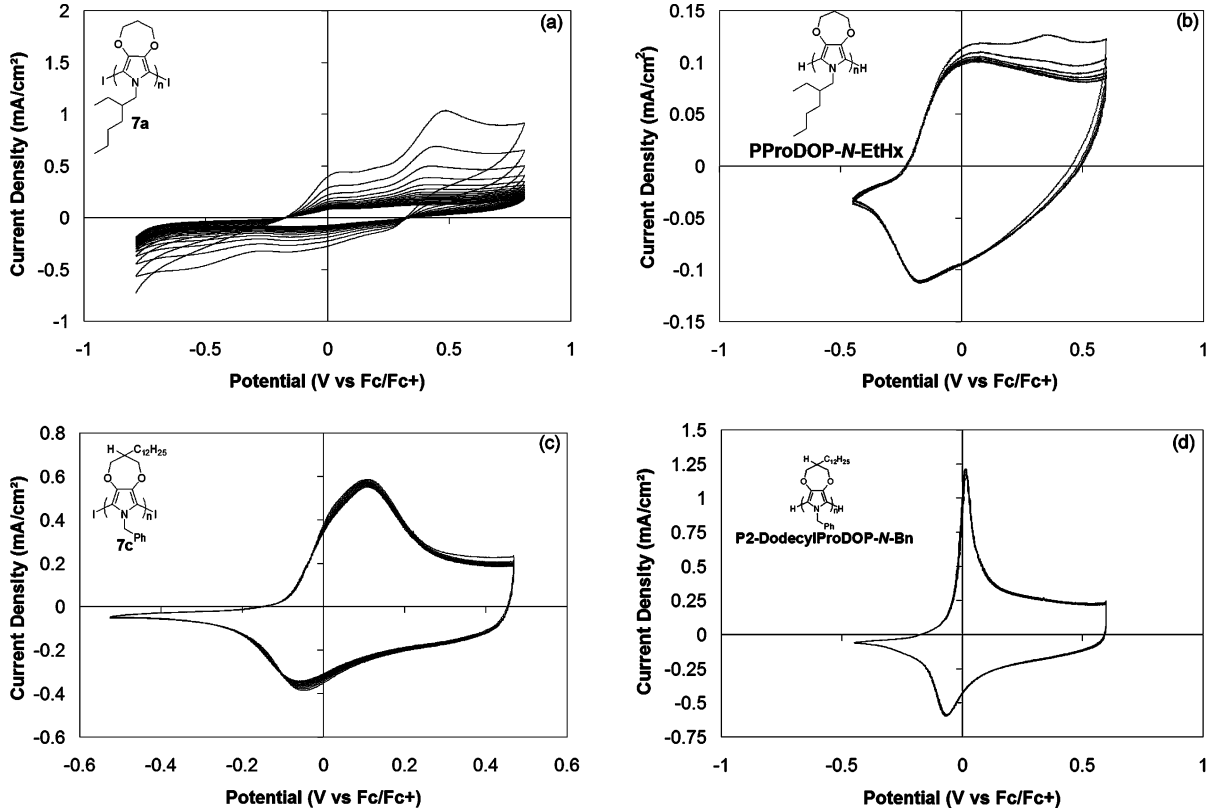

Figure 6. Repeated cyclic voltammograms in propylene carbonate of polymer films on a Pt button electrode. (a) Polymer **7a** drop-cast onto the electrode from a 5 mg/mL toluene solution (b) Electrodeposited PProDOP-*N*-EtHx. (a) Polymer **7c** drop cast onto the electrode from a 5 mg/mL toluene solution (d) Electrodeposited P2-DodecylProDOP-*N*-Bn. Arrows indicate the change in current density with repeated scans.

direction of change of absorption in the long and short wavelength regions. Upon further oxidation, a blue shift of the polaron peak was accompanied by an increase in absorbance in the near-IR and can be attributed of the depletion of the cation radicals and their replacement by dications. At these higher doping levels, the polymers exhibited a grayish-green to optically dense near black color. When the Commission internationale de l'éclairage (CIE) 1931 xy colorspace values were plotted, it can be seen that a range of color states emerged as a function of doping level. The reason for this is twofold. First, the bulk of the spectroscopic transitions with light doping occur in the 2−3 eV range, where the eye is particularly sensitive to small wavelength variations. Second, at higher doping levels, the lower energy transitions occur in the red region of the visible as well as the near-IR and thus produce polymer that absorbs very broadly over the entire visible region of the spectrum.

Polymer Film Oxidative Doping. To explore the potential utility of these polymers for solid-state applications, the polymers were prepared as solutions in toluene and cast as films onto electrode surfaces. To characterize the electrochemical processes of the polymer films, the polymers were drop-cast onto platinum button working electrodes and, after immersing into a solvent with supporting electrolyte, studied by repeated scan cyclic voltammetry. Figure 6 shows the cyclic voltammograms (CVs) for polymers **7a** and **7c** that were prepared by deiodination polymerization, and for comparison purposes, the CV data for electropolymerized films prepared from non-iodinated monomers are also shown. The upper and lower potential limits were set as to incorporate all peak redox processes observed. These redox processes all occur at low potentials (ca. 0 V vs the ferrocene/ferricinium, Fc/Fc^+, redox couple), illustrating the electron-rich character of the polymers. It can be seen that the ethylhexyl polymer, **7a**, exhibits two oxidation processes at ca. 0.0 and 0.5 V, and upon repeated scanning, both processes are seen to decrease in current density. These results are similar to the electrodeposited film and are thought to occur by a combination of delamination of the polymer from the electrode surface and polymer solubility. In both cases the redox processes were found to be of low current density (even upon repeated experiments) and poorly defined.

In contrast, the cast film of polymer **7c** exhibited a more distinct single redox process, and the film electrochemistry was found to be stable for many (over 20) scans. A sharp redox process was also observed in the electrochemically prepared film. It is evident that the well-defined and reproducible electrochemical processes observed for both **7c** and its electropolymerized counterpart are due to the presence of the dodecyl group.

Polymers **7a**−**d** were spray-cast as films onto indium tin oxide (ITO)-coated glass and characterized spectroscopically. Polymers **7b** and **7c** exhibited stable electrochromism in acetonitrile and were able to be characterized via spectroelectrochemistry. As shown in Figure 7, both polymers exhibited only a small absorbance in the visible region in either their doped or undoped forms. The most significant electrochromism, observed as a depletion of absorbance in the UV, is attributed to the nonplanar conformation of the neutral polymer caused by the *N*-substitution restricting π-overlap, thus blue-shifting the polymer π,π^* transition with respect to a highly planar state.[3] A near-IR electrochromism, observed especially for polymer **7b**, is an indication that doping induced polaronic and bipolaronic defects were sufficiently delocalized to overcome the barrier to rotation and form a planar polymer backbone. It was also found that polymer **7c** exhibited a higher contrast electrochromism in the UV than polymer **7b**, perhaps due to more facile ion flux.

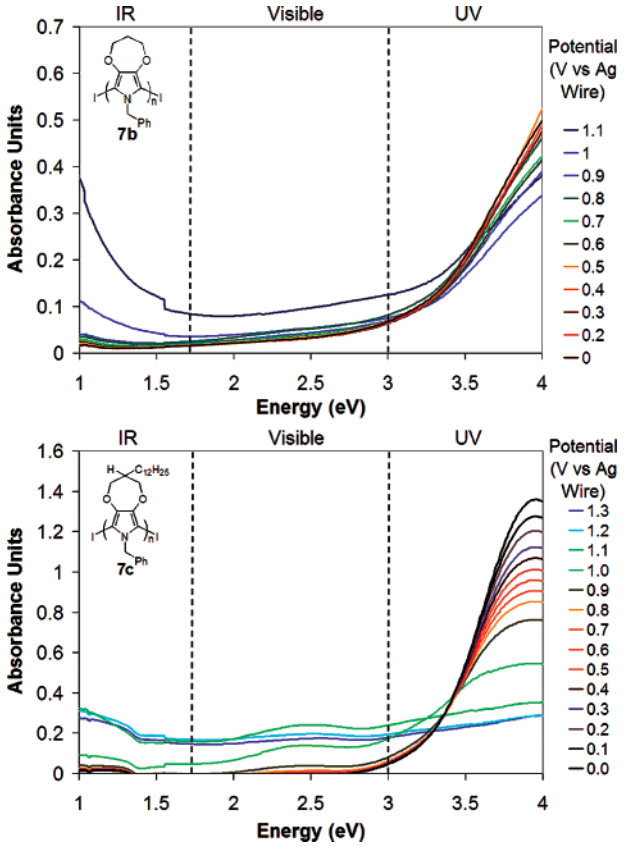

Figure 7. Spectroelectrochemistry of polymers **7b** and **7c** in tetrabutylammonium perchlorate (TBAP)/ACN. Dotted lines indicate IR, visible, and UV regions of the spectra.

Spectroelectrochemistry was not measured for polymers **7a** and **7d** because of their high solubility in all electrochemically compatible organic solvents attempted (ACN, PC, and DCM). Cast films of polymer quickly delaminated from ITO/glass before any spectroelectrochemical measurements were possible. Additionally, spectroelectrochemistry was attempted in propylene carbonate, but extremely slow film equilibration times and delamination were observed for all four polymers. It is believed that polymers **7a** and **7d** may prove useful upon further optimization of the organic solvent and electrolyte, but as will be seen below, polymer **7d** presents a highly desired compatibility in aqueous solution.

Aqueous Compatibility. It was found that polymer **7d** was the only polymer in the series able to undergo facile redox electrochemistry in aqueous solution, making it a candidate for development of electrochromic applications that utilize environmentally benign solvent systems and perhaps for use in biological sensing applications. Figure 8 shows the repeated scan polymer CV on a platinum button working electrode for polymer **7d**, which was drop-cast from toluene solution. This polymer, which was functionalized with oligoethoxy substituents, exhibited an enhanced electrochromic response in water, and in fact, the polymer was able to be switched to and from its oxidized and reduced states with only minimal loss of polymer from the substrate. It is presumed that the hydrophilic pendant groups allowed a swelling of the polymer film for facile ion flux. Furthermore, it is presumed that the oligoethoxy chains allowed for the incorporation of Li^+ cations into the polymer matrix through coordinative interactions. It is possible that these polymers could be further developed for their aqueous compatibility by optimization of the substrate and by optimizing the electrolyte.

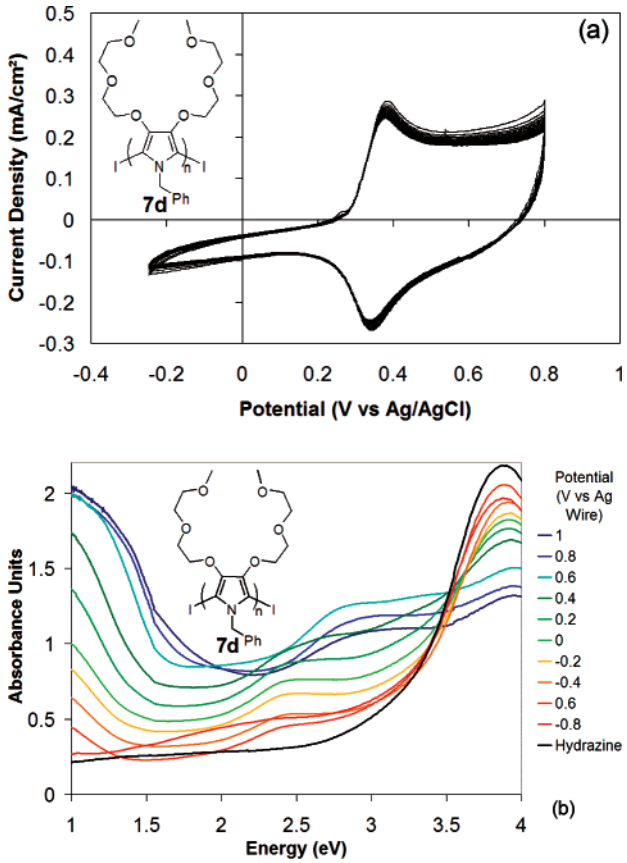

Figure 8. Aqueous compatibility studies of polymer **7d** in 0.1 M $LiClO_4/H_2O$. (a) Repeated scan electrochemistry (20 scans) of a drop-cast film on a Pt button. (b) Spectroelectrochemistry of a spray-cast film on ITO.

To further exemplify the enhanced aqueous compatibility of polymer **7d**, a film was spray-cast from toluene onto a transparent ITO/glass electrode and characterized via spectroelectrochemistry. Polymer **7d** exhibited facile spectroelectrochemistry in aqueous solution. It can be seen in Figure 8 that a relatively thick film (absorbance at $\lambda_{max} \sim 2.1$) was able to be switched, and high-contrast electrochromism was present in the visible and near-IR. This ease of solution casting from organic solvents combined with stable electrochromism in aqueous solution is unprecedented for an anodically coloring polymer and thus shows potential for further development. Because of the metal chelating nature of the oligoethoxy pendant groups, it is presumed that chelation of metal cations combined with their hydrophilicity allowed for very sharp and well-defined aqueous electrochemistry. However, this same effect would presumably make chemical polymerization of the 2,5-unsubstituted monomer with metal oxidants such as $FeCl_3$ impossible due to the inability to remove the metal after polymerization. The novel deiodination polymerization methodology described in this work provides a convenient route for the synthesis of polymers such as **7d** that would otherwise be prove to be problematic.

Conclusions

In summary, a new method for the synthesis of PXDOP-based polymers has been developed by utilizing an iododecarboxylation and deiodination polymerization methodology. This method is effective at generating high molecular weight polymer on a multigram scale without the use of metals, oxidants, solvents, or other additives. The polymers generated with this method were found to be electroactive and electrochromic in

both nonaqueous and aqueous environments. Because this polymerization method does not use metals needing removal after the reaction, it allows for the synthesis of a more diverse library of compounds. Future work may entail comparing metal-mediated polymerization procedures with the noncatalyzed procedures detailed in this work.

Experimental Section

Materials, instrumentation, and detailed synthetic procedures are described in the Supporting Information.

Acknowledgment. Ciba Specialty Chemicals is gratefully acknowledged for the funding of this project. Dr. June-Ho Jung is also acknowledged for his helpful discussions.

Supporting Information Available: Experimental conditions for the synthesis of monomers and polymers as well as the conditions for electrochemical and spectroscopic characterizations. This material is available free of charge via the Internet at http://pubs.acs.org.

References and Notes

(1) Skotheim, T. A., Reynolds, J. R., Eds. *Handbook of Conducting Polymers,* 3rd ed.; CRC Press: Boca Raton, FL, 2007.
(2) Kim, I. T.; Lee, J. Y.; Lee, S. W. *Chem. Lett.* **2004**, *33* (1), 46−47.
(3) Walczak, R. M.; Reynolds, J. R. *Adv. Mater.* **2006**, *18* (9), 1121−1131.
(4) Merz, A.; Graf, S. *J. Electroanal. Chem.* **1996**, *412* (1−2), 11−17.
(5) Merz, A.; Haimerl, A.; Owen, A. J. *Synth. Met.* **1988**, *25* (1), 89−102.
(6) Merz, A.; Kronberger, J.; Dunsch, L.; Neudeck, A.; Petr, A.; Parkanyi, L. *Angew. Chem., Int. Ed.* **1999**, *38* (10), 1442−1446.
(7) Zong, K.; Reynolds, J. R. *J. Org. Chem.* **2001**, *66* (21), 6873−6882.
(8) Meng, H.; Perepichka, D. F.; Bendikov, M.; Wudl, F.; Pan, G. Z.; Yu, W.; Dong, W.; Brown, S. *J. Am. Chem. Soc.* **2003**, *125* (49), 15151−15162.
(9) Merz, A.; Schropp, R.; Lex, J. *Angew. Chem., Int. Ed.* **1993**, *32* (2), 291−293.
(10) Schottland, P.; Zong, K.; Gaupp, C. L.; Thompson, B. C.; Thomas, C. A.; Giurgiu, I.; Hickman, R.; Abboud, K. A.; Reynolds, J. R. *Macromolecules* **2000**, *33* (19), 7051−7061.
(11) Soenmez, G.; Schwendeman, I.; Schottland, P.; Zong, K.; Reynolds, J. R. *Macromolecules* **2003**, *36* (3), 639−647.
(12) Kumar, A.; Reynolds, J. R. *Macromolecules* **1996**, *29* (23), 7629−7630.
(13) Welsh, D. M.; Kloeppner, L. J.; Madrigal, L.; Pinto, M. R.; Thompson, B. C.; Schanze, K. S.; Abboud, K. A.; Powell, D.; Reynolds, J. R. *Macromolecules* **2002**, *35* (17), 6517−6525.
(14) Cirpan, A.; Argun, A. A.; Grenier, C. R. G.; Reeves, B. D.; Reynolds, J. R. *J. Mater. Chem.* **2003**, *13* (10), 2422−2428.
(15) Reeves, B. D.; Grenier, C. R. G.; Argun, A. A.; Cirpan, A.; McCarley, T. D.; Reynolds, J. R. *Macromolecules* **2004**, *37* (20), 7559−7569.

MA071589Q